

INTEGRAL Spectroscopy of IRAS 17208-0014: Implications for the Evolutionary Scenarios of Ultraluminous Infrared Galaxies¹

Santiago Arribas^{2,3} & Luis Colina⁴

ABSTRACT

New integral field optical fiber spectroscopy obtained with the INTEGRAL system, together with archival *HST* WFPC2 and NICMOS images, have been used to investigate the ultraluminous infrared galaxy IRAS 17208–0014, one of the coldest and most luminous objects in the IRAS 1 Jy sample.

We have found that the optical nucleus is not coincident with the true (near-IR and dynamical) nucleus, but it is displaced by 1.3 kpc (1.5'') from it. As a consequence, the previous optical spectral classifications for the nucleus of this galaxy have to be revised and changed from HII to LINER. The ionized gas emission is concentrated around the optical nucleus, where a young (5-6 Myr), massive ($3\pm 1 \times 10^8 M_{\odot}$), and luminous ($6\pm 2 \times 10^{10} L_{\odot}$) starburst is detected. Contrary to what is found in *dynamically young* ULIRGs, no strong line emission tracing star-forming regions, or tidal-dwarf galaxies, is detected in the inner parts of the tidal tails.

The 2D gas velocity field identifies the *optically faint* K-band nucleus as the dynamical nucleus of the galaxy, and shows that the 3 kpc, tilted ($i \sim 35$ degree) disk is rotating at $\Delta V \sin i = 250 \text{ km s}^{-1}$. Radial motions of gas are found along the minor kinematic axis which, according to the geometry of the system, are well interpreted as inflow perpendicular to the inner disk. The existence of such inflows supports the idea that, as a consequence of the merging

¹Based on observations with the William Herschel Telescope operated on the island of La Palma by the ING in the Spanish Observatorio del Roque de los Muchachos of the Instituto de Astrofísica de Canarias. Based also on observations with the NASA/ESA Hubble Space Telescope, obtained at the Space Telescope Science Institute, which is operated by the Association of Universities for Research in Astronomy, Inc. under NASA contract number NAS5-26555.

²Space Telescope Science Institute, 3700 San Martin Drive, Baltimore, USA (arribas@stsci.edu). Affiliated with the Space Telescope Division, Research and Science Support Department of ESA.

³On leave from the Instituto de Astrofísica de Canarias – Consejo Superior de Investigaciones Científicas (CSIC)

⁴Instituto de Estructura de la Materia, Consejo Superior de Investigaciones Científicas (CSIC), Serrano 121, 28006 Madrid, Spain (colina@isis.iem.csic.es)

process, gas is channeling from the external regions, several kpc away, into the nuclear regions where the massive starburst reported above is taking place.

The kinematical, morphological, and photometric evidence presented here supports the idea that in IRAS 17208-0014 we are witnessing a luminous, cool ULIRG which is at the final coalescence phase of a system composed of two spirals with $m \leq m^*$, a mass ratio of $\sim 2:1$, each consisting of a disk+bulge internal structure, that have been involved in a prograde encounter. This system will most likely evolve into an intermediate-mass ($\sim L^*$) elliptical. The multifrequency empirical evidence gathered so far shows no trace of a luminous QSO, and indicates that starbursts dominate the energy output in this galaxy. Therefore IRAS 17208–0014 does not follow the behavior expected in the ‘ULIRG to QSO’ evolutionary scenario proposed by Sanders et al., but support the one recently proposed by Colina et al, where two low mass disk galaxies would produce luminous cool ULIRGs that would not evolve into a QSO phase.

The present study illustrates some caveats to bear in mind when studying high- z galaxies lacking 2D spectral information of adequate linear resolution, and shows that near and mid-IR integral field spectroscopy is needed to derive the relevant astrophysical quantities.

Subject headings: galaxies: active — galaxies: nuclei — galaxies: interactions
— galaxies: starburst — galaxies: individual (IRAS 17208-0014)

1. INTRODUCTION

Ultraluminous Infrared Galaxies (ULIRGs) are the most luminous objects in the local universe, with bolometric luminosities $L_{bol} \approx L_{IR} \geq 10^{12} L_{\odot}$. Having large amounts of gas and dust, they are undergoing an intense starburst activity triggered by interactions and/or mergers. This starburst activity is believed to be their major energy reservoir (Genzel et al. 1998), though the relative importance of the AGN phenomenon as energy power in ULIRGs is under debate (e.g. Sanders and Mirabel 1996). Sanders et al. 1988 suggested an evolutionary sequence according to which ULIRGs are the precursors of optical quasars. In this scenario, *warm* ULIRGs (i.e. $f_{25\mu}/f_{60\mu} > 0.2$) are in a later evolutionary stage than *cool* ULIRGs ($f_{25\mu}/f_{60\mu} < 0.2$). High spatial resolution imaging and nuclear spectroscopy have found evidence in support of this scenario (e.g. Surace et al. 1998; Veilleux, Kim, Sanders 1999 and references there in). On the other hand, Genzel et al (2001) have found that most ULIRGs seem to be evolving towards intermediate-mass

(L*) elliptical galaxies, suggesting that ULIRGs mergers are ellipticals in formation. However, details on how the ULIRGs evolve remain very uncertain despite the progress made recently in characterizing merger evolution on the basis of theoretical models (see Mihos & Hernquist, 1996; Naab & Burkert, 2001 and references therein). These studies show that gas dynamics and star formation in mergers are closely related. They also indicate that the internal structure of the merging galaxies as well as their mass ratio are key factors in determining the characteristics of ultraluminous infrared galaxies.

From an observational point of view, detailed studies of the complex kinematics and ionization structures of these objects demand the analysis of their spectral properties in two dimensions (see also Murphy et al. 2001). However, only a very limited number of this type of studies exists so far (e.g. Mihos & Bothun 1998; Wilman, Crawford, Abraham 1999). We have recently started a program aimed at studying a representative sample of ULIRGs combining Integral Field Spectroscopy (IFS) and high resolution *HST* imaging. Some of the main results obtained so far for other ULIRGs such as Mrk 273, IRAS 12112+0305, IRAS 08572+3915, Arp 220, and IRAS 15206+3342 can be found elsewhere (see Arribas & Colina 2002, and references there in).

In this paper, we present new INTEGRAL spectroscopy and archival *HST* imaging of IRAS 17208-0014. This is an ultraluminous infrared galaxy with some interesting properties. Despite being the second most luminous galaxy in the sample studied by Kim et al. (1995) ($L_{bol} = 10^{12.4} L_{\odot}$), it does not show evidence of an AGN. In particular, i) it has been reported as a case of a HII/starburst excitation in the optical (Veilleux et al. 1995), and in the mid-infrared (Lutz, Veilleux & Genzel 1999), ii) the nucleus in the near and mid infrared images is extended ($\sim 2''$; Scoville et al. 2000; Soifer et al. 2000), and iii) the near infrared search for a hidden broad-line indicated no signs of BLR (Goldader et al. 1995). *HST*-NICMOS observations (Scoville et al. 2000) have revealed the presence of at least 18 clusters of star formation, mainly concentrated in the inner regions, where extinction is high. The presence of a rotating disk of molecular gas has been inferred from CO observations (Downes & Solomon 1998). The nucleus also has one of the strongest known OH megamasers, and a radio continuum source of ~ 250 pc in size (Martin et al. 1989).

Ground based optical imaging of IRAS 17208-0014 (Murphy et al. 1996; Duc, Mirabel, Maza, 1997) has revealed a disturbed and irregular system with two prominent tidal tails towards the SE and NW extending to distances larger than 20 kpc. This morphology, together with the fact that near infrared images show a luminosity profile typical of ellipticals, have lead to the suggestion that this is a case where an elliptical galaxy is being formed after a disk-disk collision (Duc, Mirabel, Maza, 1997). Furthermore, IRAS 17208-0014 is located near the Fundamental Plane (FP), in a region populated by fast

rotating ellipticals and lenticulars with intermediate mass, and disk isophotes (Genzel et al 2001). This result also suggests that the merger is in a relatively advanced phase, and will eventually lead to an elliptical of the above mentioned characteristics.

The new optical INTEGRAL spectroscopy and *HST* imaging presented here (Sect. 2) will be used to characterize the stellar structure (Sect. 3.1), the ionized gas morphology and excitation (Sect. 3.2), the properties of the extra-nuclear starburst (Sect. 3.3) and the 2D kinematics of the ionized gas (Sect. 3.4) in this galaxy. On the basis of these results and previous published studies, we will discuss in Section 4 the properties and evolutionary phase of the merging system, as well as the implications for studies of high-*z* galaxies. Finally, in Section 5, the main results are summarized.

At the assumed distance of 183 Mpc for IRAS 17202-0014, one arcsec corresponds to a linear size of 888 pc. Throughout the paper, a Hubble constant of $70 \text{ kms}^{-1} \text{ Mpc}^{-1}$ is assumed.

2. OBSERVATIONS AND DATA REDUCTION

Integral field spectroscopy of IRAS 17202-0014 was obtained with the INTEGRAL system (Arribas et al. 1998) connected to WYFFOS (Wide Field Fiber Optic Spectrograph; Bingham et al. 1994) on the 4.2m William Herschel Telescope during 1999 April 3. The bundle of fibers SB2 (Standard Bundle number 2), consisting of 219 fibers, each $0.9''$ in diameter, was used. This is arranged such that 189 fibers cover a rectangular area of $16.5'' \times 12.3''$ ($14.6 \text{ kpc} \times 10.9 \text{ kpc}$ at the distance of IRAS 17202-0014) while 30 additional fibers, forming a ring of $90''$ in diameter concentric with the rectangle, measure simultaneously the sky background (see Arribas & Mediavilla 2000 for further details on integral field fiber spectroscopy). The spectra were taken using a 600 line/mm grating with an effective resolution of 4.8 \AA and covering the $5000\text{-}7900 \text{ \AA}$ spectral range. The total integration time was 7800 seconds split into 4 separate exposures, with seeing of about $1.1''$.

Data reduction followed the standard procedures applied to spectra obtained with two-dimensional fiber spectrographs (see, for instance, Arribas & Mediavilla 2000, and references therein). As an example, the two-dimensional distribution of the reduced spectra in the range of the redshifted $\text{H}\alpha + [\text{NII}] + [\text{SII}]$ lines (i.e. $6792 - 7045 \text{ \AA}$) are presented in Figure 1. $\text{H}\beta$ and the $[\text{OIII}]\lambda\lambda 4959, 5007$ appeared conspicuously in only four spectra: 102, 103, 104, and 107 (not shown).

For each spectrum, the radial velocities and velocity dispersions were measured by adjusting Gaussian functions to the observed emission line profiles using the DIPSO

package (Howarth & Murray 1988). The uncertainties associated with the individual velocities are estimated to be in the order of $\pm 15 \text{ km s}^{-1}$. The velocity dispersion values presented in this paper are corrected from instrumental profile and redshift.

The archival *HST* images of IRAS 17208-0014 obtained in the I-band (F814W filter, WFPC2) and K-band (F222M, NIC2) were originally taken as part of programs 6346 (PI: K. Borne) and 7116 (PI: N. Scoville), respectively. The total exposure time for the F814W image was 800 seconds divided into two identical exposures of 400 seconds each, using the CR-SPLIT option. The data were recalibrated at the time of dearchiving using on-the-fly calibration software and the best reference calibration files available. The NICMOS F222M image, first analysed and published in Scoville et al. 2000, with a total integration time of 288 seconds, was recalibrated in October 2002 with *calnica* and *calnicb* with the best available reference files.

3. RESULTS

3.1. Stellar structure and differential extinction effects

The INTEGRAL red continuum image taken with a narrow 7029-7068 Å window (Fig. 2, bottom-left panel) has a good morphological resemblance to the WFPC2 I-band image (Fig. 2, upper-left panel). This allows us to establish the absolute positioning of the INTEGRAL maps with an uncertainty of about $0''.3$ with respect to the *HST* reference frame. In addition, the WFPC2 and NICMOS images could be placed on the same coordinate system using point-like structures present in both images.

The morphology of the outer low-surface brightness region in the red continuum images is like that of a perturbed elliptical. However, inwards, the presence of spiral arm-like structures are rather conspicuous. The innermost star-forming clusters previously identified in the near-IR with NICMOS (Scoville et al., 2000; see also Fig. 3) are also detected in the WFPC2 I-band image. Leaving aside the contribution of the circumnuclear clusters, the inner isophotes in the infrared images define an elliptical structure, suggesting the presence of a tilted disk with $i = 35 \pm 15$ degrees and 3 ± 0.5 kpc in diameter (Fig. 3).

There is a general consensus that ULIRGs are galaxies where most of their active regions, either massive starbursts or AGN, are enshrouded in dust. However, the dust distribution, although concentrated towards the nuclear regions, i.e. inner few kpcs, is very patchy and therefore differential extinction effects play a major role in interpreting the results (e.g. Colina et al. 2001). In IRAS 17208–0014, the most relevant effect of the differential extinction is that the true nucleus of the galaxy does not coincide with the region identified

as the nucleus in the optical, but it is located about 1.5 arcsec (1.3 kpc) southwest of it (compare Fig.2 upper-left with Fig. 3). In the direction of the optical nucleus, the hydrogen recombination lines (see next section) in the INTEGRAL spectra indicate an extinction A_v of about 5.5 magnitudes, in good agreement with previous measurements (see Table 1). No $H\beta$ is detected towards the near-IR nucleus. However, assuming that extinction is in a foreground screen (i.e. not mixed with the stars), and using the law derived by Rieke and Lebofsky (1985) an extinction of up to $A_v = 8$ magnitudes is inferred from the infrared colors (Scoville et al 2000). However, this could be a lower limit. Scoville et al. pointed out that the nuclear power source in IRAS 17208–0014 could be buried even at near-infrared wavelengths.

A secondary emission peak in the optical, located at about $3''$ (2.7 kpc) southeast of the optical nucleus, is rather clear in both the INTEGRAL and the WFPC2 images. This region could, in principle, be identified as the second nucleus of a merging pair. However, its flux loses strength at longer infrared wavelengths, and nearly disappears in the $2.2 \mu\text{m}$ map (Fig. 3), suggesting that its optical emission is associated with a relatively young population located on one of the spiral arm-like structures.

3.2. Ionized gas morphology and excitation structure

The structure of the warm ionized gas is traced here by the $H\alpha$ map (Fig. 2, central upper panel). This image shows a bright nucleus and a low intensity extended emission of at least 8 kpc elongated in the SE - NW direction. The structure of the outer envelope is reminiscent of that of the stellar component, though it does not have a one-to-one correspondence. In fact, the ionized gas emission is more compact and it extends towards the North, where a tidal tail is observed in deep optical continuum images (see, Murphy et al. 1996; Duc, Mirabel, Maza, 1997). However, no strong line emission tracing star-forming regions or tidal-dwarf galaxies is observed in the inner parts of the tidal tails, as found in some double-nuclei ULIRGs (e.g. IRAS 12112+0305: Colina et al. 2000; IRAS 08572+3915: Arribas, Colina, Borne 2000; IRAS 14348–1447: Monreal et al., in preparation).

The ionized gas in the optical nucleus exhibits excitation conditions characteristic of HII regions (see Table 1 and Fig. 2). Strong $H\alpha$, relative to [NII], is also detected towards the south of the optical nucleus. However, apart from these regions, the [NII] emission is at least as intense as $H\alpha$ in the rest of the regions (see Fig. 1). Further support for this dichotomy in the excitation conditions comes from the ratio [SII]/ $H\alpha$, which has a minimum in the optical nucleus, and is considerably higher elsewhere (see Fig. 1 and

compare, for instance, spectra 103 and 100). $H\beta$ and [OIII] are detected in only a few spectra outside the optical nucleus, with a ratio of [OIII]/ $H\beta \sim 0.5$. Note that for a [OIII]/ $H\beta$ ratio lower than 1, the values of the [OI]-, [NII]-, and [SII]-to- $H\alpha$ ratios, almost unaffected by internal extinction, are good discriminators between LINER and HII ionization (Veilleux & Osterbrock, 1987). Therefore, our new INTEGRAL spectroscopy shows that outside the optical nucleus, the excitation properties of the ionized gas are characteristic of LINERs (see Table 1 and Fig. 2). This includes the near-IR nucleus (i.e. true nucleus, see § 3.4), which is therefore classified as a LINER (Table 1). Since previous classifications were based on long-slit spectroscopy of the optical nucleus (Veilleux et al, 1995), the classification of the nucleus of IRAS 17208–0014 has to be revised and changed to LINER. This new classification is not in contradiction with the classification as a starburst based on ISO spectroscopy (Lutz, Veilleux, and Genzel, 1999), especially if we take into account the different spatial resolution. On the contrary, as pointed out by these authors, rather than indicating the presence of an active nucleus, the LINER spectra in ULIRGs are more likely due to shocks produced by compact and massive starbursts.

3.3. Massive extranuclear starburst

The properties of the optical emission peak, i.e. the optical nucleus, indicate that a massive, young, starburst is taking place in an extranuclear region (see § 3.4). The strong hydrogen recombination lines with equivalent widths of $94 \pm 10\text{\AA}$ and $13 \pm 3\text{\AA}$ for $H\alpha$ and $H\beta$, respectively, indicate the presence of a young burst of about 5 to 6 million years. Considering an age of 6 Myrs, the dereddened $H\alpha$ luminosity (see Table 1), and the WFPC2 I-band absolute magnitude ($M_I = -21.7$, if $A_V = 5.5$ mag. is assumed) can be used to obtain two independent estimates of the total mass in the burst. Assuming the predicted $H\alpha$ and I-band luminosity for an instantaneous burst characterized by a Salpeter initial mass function and stellar masses in the 1 to 100 M_\odot range (STARBURST99; Leitherer et al. 1999), the two estimates agree and give a total mass of $3 \pm 1 \times 10^8 M_\odot$. The bolometric luminosity of such a young and massive starburst is $6 \pm 2 \times 10^{10} L_\odot$. Thus, although very massive, this starburst still produces a small fraction of the energy output of IRAS 17208–0014, equivalent to 2.5% of its IR luminosity. The region where this starburst is located has a size of about 0.9 kpc in diameter. Therefore, it is likely that this starburst, as suggested by the *HST* images, does not form a single entity but is distributed in several less massive clusters. In this respect, most of the bright clusters identified in the near-IR are located in this region (Scoville et al. 2000). In particular, the two first-ranked K-band clusters alone (clusters 1 and 9 in Scoville et al. 2000) produce a combined bolometric luminosity of $2 \times 10^{10} L_\odot$, i.e. a factor of three less than the luminosity of the

starburst, if the same age and extinction as measured for the entire region is assumed.

3.4. Kinematic tracing of the dust-enshrouded dynamical nucleus and inner gas disk

The velocity field of the ionized gas inferred from the $H\alpha+[NII]$ lines is shown in Figure 2 (bottom-right panel). The largest velocity gradient is not found across the optical nucleus, but across the infrared nucleus (see also Fig. 3, bottom). This indicates that the dynamical nucleus is in positional agreement with the infrared nucleus. Therefore, even if the nuclear power source is buried at near infrared wavelengths, the infrared nucleus indicates its direction. Note that the highly symmetric pattern of the ionized gas velocity field allows us to accurately locate the position of the true nucleus using optical spectroscopy (i.e without the need of near-IR observations).

The peak-to-peak velocity difference corresponds to $\Delta V \sin i = 250 \text{ km s}^{-1}$ along $PA \sim 130$ degrees. This direction is in good agreement with that of the major photometric axis inferred from the inner isolines in the NICMOS images (excluding the effects from the clusters; see Fig. 3). The agreement between the photometric and kinematic axes suggests that we are observing a rotating disk of ionized gas. The kinematic axes of this disk are also in good positional agreement with those of the molecular (CO) disk found by Downes and Solomon (1998). It is also worth noting that the velocity field does not show any evidence for the presence of a second nucleus.

Outside the inner disk the iso-velocities twist, having a characteristic S-shape. Although this may indicate warps (e.g. Mediavilla et al. 1991), we believe it is due to the transition from inner-disk to outer-envelope seen in projection, as suggested by fact that the isovelocity distortions appear at the edge of the inner disk.

The velocity dispersion map indicates relatively large velocity dispersions over most of the observed region (i.e. FWHM $\sim 300 \text{ km/s}$). Within uncertainties, the infrared nucleus is in positional agreement with a local maximum ($\sim 450 \text{ km/s}$) in the velocity dispersion map (Figure 3), which in turn is well centered with the kinematic center of rotation. Therefore, there is little doubt that the dynamical nucleus of the galaxy is located there. Another local maximum in the velocity dispersion map is observed towards the SW at about 3 arcsec (2.7 kpc). The mean velocity of this region is redshifted by about 200 km/s with respect to the systemic, as can be observed in the velocity field map. These redshifted velocities are found in a position near the kinematic axis, where mainly systemic velocities are expected for a purely rotating disk. This indicates the presence of a kinematically distinct component.

4. DISCUSSION

4.1. Tidal-induced inflows

In principle, the kinematically distinct component reported in §3.4 could indicate the presence of large-scale outflows originated by AGN-driven jets (Colbert et al. 1998 and references therein). However, the fact that no evidence for either an AGN or a jet has been reported for this object makes this explanation rather speculative. Superwinds (Heckman et al. 1990) could also be, in principle, a possible explanation. However, if the spiral-like arms observed in optical images are trailing, the INTEGRAL velocity field of the inner disk (i.e. redshifted velocities in the SE; blueshifted velocities in the NW) indicates that the closer part of the disk is in the NE. With this geometry, and assuming an inclination of 35 degrees (as suggested by the inner isolines in the NICMOS K image), two outflowing components are expected to be seen in projection over the SW and another two over the NE (see the geometry described in Figure 17 of Heckman et al. 1990). In the SW, the component closest to us should have blueshifted velocities. The farthest component seen in projection over the SW could have blueshifted or redshifted velocities depending on the opening of the outflow cone. The fact that we only observe one extra component (out of four expected) which also has relatively strong redshifted velocities along the SW part of the minor axis makes the superwind scenario very unlikely in the case of IRAS17208-0014.

Alternatively, the kinematically distinct component could be associated with streaming motions of gas related to the merging process. The fact that these motions are found along the minor axis suggests that they are perpendicular to the disk of gas. Taking into account the geometry of the inner disk (i.e. with NE being the closer part, $i=35$ degrees), the observed redshifted velocities along the SW part of the rotation axis imply inflow. (Conversely, outflows along the SW part of the rotation axis would imply approaching velocities, i.e. a blueshifted component). Note that the rotation axis is a canal where mass can travel efficiently towards the innermost parts of the galaxy without the limitations imposed by the conservation of angular momentum. In short, the extra redshifted component found along the SW part of the minor axis can be explained as the result of an inflow motion perpendicular to the disk. Even if the inflows may lose efficiency at the innermost regions (i.e., the inner kpc), their existence supports the idea that, as a consequence of the merging process, gas is channeling from the external regions, several kpc away, into the nuclear regions where the massive starburst described in § 3.3 is taking place. The presence of strong inflows and associated star formation are expected during the final coalescence phase of two disk galaxies with bulges (Mihos and Hernquist, 1996). IRAS 15206+3342 (Arribas & Colina 2002) is another case where these type of motions are clearly observed.

4.2. IRAS 17208–0014 Near-IR Luminosity: Extinction Corrections for ULIRGs

The measurements of the luminosity of ULIRGs in the near-infrared and the internal extinction corrections to be applied are not well defined. Some authors (Genzel et al. 2001) argue that extinction over the entire size of these galaxies is very large and therefore corrections to the integrated apparent magnitudes, even in the K-band, are not negligible, i.e. mean corrections of 0.7 mag have to be applied. Others (Colina et al. 2001) indicate that dust distribution is very patchy in ULIRGs and therefore while internal extinction towards the nucleus can be high, the mean extinction over the entire ULIRG is much less due to large differential extinction gradients. In the following, we discuss the differential extinction in IRAS 17208–0014 and show how this extinction should be taken into account in order to obtain a reliable near-IR luminosity of this galaxy, and of ULIRGs in general.

In IRAS 17208–0014, NICMOS colors (Scoville et al. 2000) and the INTEGRAL spectroscopy presented here (see §3.1) indicate visual extinctions of about 8 and 5.5 mag towards the near-IR nucleus and the extranuclear starburst (i.e. “optical nucleus”), respectively. However, the mean extinction across the entire galaxy appears to be much less as indicated by the bluer near-IR colors (Scoville et al. 2000) when increasing the size of the aperture from 1"1 to a 11"4 diameter (i.e. from 1 to 10 kpc at the assumed distance for IRAS 17208–0014). Stellar populations cover a limited and well defined range of near-IR colors with almost constant J–H of about +0.8 and H–K of +0.35 for starbursts older than 10 Myr, and slightly bluer colors for younger starbursts (STARBURST99; Leitherer et al. 1999). Therefore, the observed, integrated colors can be used to estimate the mean extinction within the galaxy. For IRAS 17208–0014, the NICMOS J–H and H–K colors measured within an aperture of 11"4 or 10 kpc (i.e. covering the field-of-view of our INTEGRAL spectra) are +1.3 and +0.6, respectively, and therefore the mean extinction (A_V) is about 2.5 mags, much less than for the nuclei. Therefore, the extreme extinctions measured in the nuclear regions (~ 1 kpc) through small apertures can not be applied to the entire galaxy.

This fact is obviously important when computing the absolute near-IR magnitudes of ULIRGs in general, and of this galaxy in particular. The observed apparent H-band magnitude of 12.09 in a region of 10 kpc in diameter, i.e. including the nucleus and host (Scoville et al. 2000), corresponds to an absolute magnitude of $M_H = -24.22$ (i.e. an L^* galaxy) if no reddening correction is applied. If the mean extinction of $A_V = 2.5$ mag is considered for the entire galaxy, the corresponding luminosity of the system is $1.5L^*$.

4.3. Characteristics of the Merger

The morphological and kinematical properties of IRAS 17208–0014 indicate that this system is in an advanced phase of the merging process between two gas-rich galaxies. The predicted strong inflow (and associated star formation) in this phase is well detected in the case of IRAS 17208–0014, as we have discussed in § 4.1 (and § 3.3). High-resolution NICMOS images (Scoville et al. 2000, see also Fig. 3) and INTEGRAL two-dimensional kinematics do not show evidence for a second nucleus. The massive young clusters are preferentially located in the circumnuclear regions (i.e. inner 1-2 kpc) with no signs of star forming regions along (the observed inner parts of) the tidal tails, like those found in dynamically younger systems where two distinct nuclei are still present (e.g. IRAS 12112+0305, Colina et al, 2000; IRAS 08572+3915, Arribas, Colina, Borne 2000; IRAS 14348–1447, Monreal et al. in preparation). Further morphological characteristics, e.g. $\sim r^{1/4}$ intensity profile in the near-IR (Scoville et al. 2000), also indicate that IRAS 17208–0014 is indeed an advanced merger/elliptical in formation.

The fairly regular disk kinematics shown in our velocity field (as well as the good alignment of the kinematic and photometric axes) points to an unequal-mass merger according to the numerical simulations by Bendo and Barnes (2000) and Naab and Burkert (2001). This is supported by recent measurements of the central V_{rot}/σ ratio from stellar kinematic data (Genzel et al. 2001). The value V_{rot}/σ of 0.48 indicates that the merger product is a relatively fast rotator and therefore that the mass ratio of the two progenitor galaxies involved in the merger should be $\sim 2:1$. Moreover, the relatively long (though faint) tidal tails in IRAS 17208-0014 suggest that the encounter could have been prograde (Dubinski, Mihos & Hernquist 1999).

The estimated dereddened H-band luminosity of IRAS 17208–0014 corresponds to $1.5L^*$ (see §4.2). This result by itself does not imply that the system is the merger of two massive spirals (i.e. $\geq m^*$). In fact, young (6 to 10 Myr) starbursts have H-band M/L ratios a factor of 50 lower than that of old 1 Gyr stellar populations. In other words, the same H-band luminosity will be produced by an old bulge population and by a 50 times less massive young starburst. As an example, the massive extranuclear starburst of $3 \times 10^8 M_{\odot}$ (see §3.3) alone produces an H-band luminosity of $0.1 L^*$. Moreover, a continuous $100 M_{\odot} \text{ yr}^{-1}$ star formation over 10-20 million years, inferred to be happening in ULIRGs in general, produces an L^* luminosity in the H-band. Recent stellar kinematical measurements support low M/L values. In fact, IRAS 17208–0014 is located near the region of the Fundamental Plane (FP) populated by intermediate-mass ($\sim L^*$) ellipticals, and its dynamical mass corresponds to $1.1 \times 10^{11} M_{\odot}$, or $0.8m^*$, from stellar velocity dispersion measurements (Tacconi et al. 2002). Although the gas kinematics may not

necessarily trace the dynamical mass, we note that the present gas velocity dispersions are only somewhat lower than the stellar values which also suggests a mass lower than m^* for the system. These results therefore support the scenario proposed by Colina et al. (2001) where cool ULIRGs like IRAS 17208–0014 would be produced during the coalescing of two low-mass disk galaxies.

In summary, the kinematical, morphological, and photometric evidence presented here supports the idea that we are witnessing in IRAS 17208-0014 a luminous, cool ULIRG which is at the final coalescence phase of a system composed of two low mass spirals (i.e. $\leq m^*$), with a mass ratio of 2:1, each consisting of a disk+bulge internal structure, that have been involved in a prograde encounter. This system will most likely not evolve into a luminous QSO (see next section), but into a fast rotating elliptical ($\sim L^*$).

4.4. IRAS 17208–0014: A Cool ULIRG not Evolving into a Luminous QSO

According to the evolutionary scenario first proposed by Sanders et al. (1988), cool ULIRGs would evolve into warm ULIRGs, and finally into QSOs. This scenario implies that cool ULIRGs should be found preferentially among galaxies in the initial and intermediate phases of the merging process while the galaxies involved in the collision still preserve much of their individual identities, or are separated enough that their nuclei have not merged yet. On the other hand, warm ULIRGs should be found in late phases and therefore preferentially among close pairs, or even single-nucleus galaxies, while QSOs should be located exclusively in compact, single nucleus systems.

According to this scenario, IRAS 17208–0014, which is at an advanced merging phase (see § 4.3) and has an infrared luminosity of $L_{IR} = 10^{12.4} L_{\odot}$ (i.e. one of the most luminous ULIRG in the 1 Jy sample), should be showing the characteristics of a warm, QSO-like ULIRG. However, quite the opposite, IRAS 17208–0014 shows no signs for the presence of a QSO: (1) with a f_{25}/f_{60} ratio of 0.05, it is one of the coldest ULIRGs, (2) its near and mid-IR emission show the same extended structure of about $2''$ (Scoville et al. 2000; Soifer et al. 2000) with no evidence of a luminous, point-like, nuclear source, (3) there is no trace of a (dominant) AGN component from either the optical (this work), or the near (Goldader et al. 1995) and mid-IR (Lutz et al. 1999) spectroscopy, and not even from the hard X-ray (Risaliti et al. 2000). Moreover, the low f_{25}/f_{60} and F_{HX}/F_{IR} (1.25×10^{-4}) flux ratios are close to those of luminous infrared (i.e. $L_{IR} \leq 10^{11}$) starbursts, and unlike the values of luminous infrared galaxies with a Seyfert 1 nucleus (about 2 and 0.1, respectively; see figure 5 in Risaliti et al 2000). In addition, considering the dereddened $H\alpha$ luminosity for the entire galaxy (3.4×10^{42} erg s^{-1}), the ratio of hard X-ray to $H\alpha$ luminosity is 0.35,

much less than the median value of 15 for QSOs, Seyfert 1, and low-luminosity LINER 1 nuclei (Ho et al. 2001), and similar to the average measured value (0.14) in nearby nuclear starbursts (Pérez-Olea & Colina 1996). Finally, the low radio flux density of 102 mJy at 1.4 GHz (Condon et al. 1996) gives an X-ray to radio luminosity ratio of 520, also in agreement with the average value of 400 in nearby nuclear starbursts (Pérez-Olea & Colina 1996).

In addition to these energy arguments, there are also dynamical arguments indicating that, if IRAS 17208–0014 harbors a central black-hole, it must have a relatively low mass and therefore not capable of producing a luminous QSO ($M_{BH} \sim 10^9 M_{\odot}$). The estimated mass of the IRAS 17208–0014 black-hole is $2.3 \times 10^8 M_{\odot}$, based on ground-based near-infrared stellar velocity dispersion measurements and assuming the correlation between the black hole masses and bulge velocity dispersion for early type galaxies also holds for late phase ULIRGs (Tacconi et al. 2002). The stellar velocity dispersion has been measured over a region of about 1 kpc in diameter (0.5 to 1.2 effective radii as mentioned in Tacconi et al. 2002). The central gas and stellar distribution in ULIRGs differ dramatically from that of ellipticals and bulges of spirals due to their large concentrations of high density molecular gas, and young, massive stellar clusters. Therefore, it is likely that in ULIRGs, aside from the black hole itself, these stellar and gas components make a non-negligible fraction of the total mass. Therefore, the mass estimate of the nuclear black hole mass should most likely be considered as an upper limit to the true mass of the black-hole.

In summary, despite its advanced dynamical phase, starbursts seem to be the dominant energy source in IRAS 17208–0014 and, if an AGN exists, it must produce only a minor contribution to the overall energy and ionizing budget. We note that similar characteristics (i.e. advanced merger without clear evidence of QSO) have also been found in IRAS 15206+3342 (Arribas and Colina 2002). These cases do not follow the behavior expected in the ‘ULIRG to QSO’ evolutionary scenario proposed by Sanders and collaborators, therefore questioning its universality. On the other hand, if the alternative scenario proposed by Colina et al. (2001) is correct, IRAS 17208–0014 represents an example of the merger of two low mass disk galaxies that will produce a luminous, cool ULIRG but will never evolve into a QSO phase.

4.5. Implications for High-z Dust-enshrouded Massive Starburst Galaxies

There are three fundamental questions that have to be answered in the future in order to advance our knowledge of high-z galaxies: (1) what is the fraction of AGNs as a function of redshift, (2) what is the mass distribution of the pre-galactic objects in the early Universe, and (3) how do pre-galactic objects evolve into present-day galaxies (i.e.

interaction/merging rates, number of colliding objects)? The results presented for IRAS 17208–0014 illustrate the problems and caveats that have to be taken into account when investigating high- z dusty objects and before answering the above mentioned questions.

IRAS 17208–0014 is a clear example of a ULIRG where the optical nucleus, both in continuum and emission lines, does not trace the true dynamical nucleus of the galaxy but is displaced by a large amount of 1.3 kpc. Moreover, IRAS 17208–0014 shows two strong continuum peaks in the optical that could naively be associated with the nuclei of two galaxies. However, two-dimensional kinematics and K-band imaging show that none of these optical nuclei are associated with the *true single* nucleus of this galaxy. Therefore, conclusions about the morphological properties and structure of the progenitors of high- z dusty starbursts, including merging rates, interaction phase, or number of colliding objects, would depend critically on a reliable two-dimensional knowledge of the stellar structure and kinematical properties of the gas.

IRAS 17208–0014 is also an example of misleading spectral classification of its nucleus in the optical. In the past, due to the lack of two-dimensional spectroscopy, this ULIRG has been classified as an HII, while the true nucleus has a LINER spectrum, as shown here. If this is a common situation, it could have severe implications. Since the fraction of AGN in galaxies as a function of redshift can trace the formation and growth of massive black-holes at early epochs, establishing a reliable classification of the nuclei of high- z galaxies, in particular of the most common low-luminosity AGN, is obviously needed.

Regarding its kinematics, the largest velocity gradient and the velocity dispersion peak in IRAS 17208–0014 are not found towards the optical nucleus, but towards the optically faint, K-band nucleus. If the emission peak of the ionized gas is decoupled from the stellar continuum, or the stellar and gas distribution do not trace the true nucleus of the galaxy, any mass estimate from optical emission lines (e.g. H α) based on spatially unresolved velocity dispersion measurements will be affected by an undetermined error, depending on the specific object. IRAS 17208-0014 is not an isolated case among ULIRGs. Other ULIRGs for which integral field spectroscopy is available (i.e. Mkr 273: Colina, Arribas & Borne 1999; IRAS 12112+0305: Colina et al. 2000; IRAS 08572+3915: Arribas, Colina & Borne 2000; Arp 220: Arribas, Colina, Clements 2001; IRAS 15206+3342: Arribas & Colina, 2002) do show similar features, most notably the decoupling between the stellar and ionized gas structure, offsets between the velocity dispersion peak and the optical light distribution, and strong differential extinction effects that could lead to wrong conclusions if investigated without adequate spatially resolved 2D spectroscopy.

Future near and mid-IR observations of high- z dusty galaxies with large telescopes will effectively observe the rest-frame optical spectrum (0.4 - 0.7 μ m) for redshifts of three, or

larger. If, as demonstrated in this paper (see also previous papers of this series) optical IFS data is relevant for adequately interpreting the properties of local ULIRGs, so near and mid-IR IFS should be for interpreting high- z galaxies. Although sensitivity and angular resolution (which worsen with wavelength) may limit these types of studies, a good understanding of the observational effects from analyzing a representative sample of local ULIRGs seems crucial in order to grasp the limitations of poorer linear resolution and 1D studies.

5. SUMMARY:

Integral field optical fiber spectroscopy with the INTEGRAL system, together with archival *HST* WFPC2 and NICMOS images, have been used to investigate the ultraluminous infrared galaxy IRAS 17208–0014. The main results are the following:

- 1) Differential extinction plays a major role in interpreting the innermost regions of this system. The optical nucleus (in both the continuum and line emission) is not coincident with the true (near-IR and dynamical) nucleus, but is displaced by 1.3 kpc (1.5'') from it. As a consequence, the previous optical spectral classification of the nucleus of this galaxy has to be revised and changed from HII to LINER.
- 2) A mean internal extinction equivalent to 2.5 mag in the visual is derived for the galaxy. Due to the patchy structure of the dust distribution, this average extinction is much lower than the values (5.5 to 8 mag) measured in the nuclear regions. A dereddened H-band luminosity of $\sim 1.5L^*$ is found for the entire system. Most of this luminosity is dominated by the young starbursts, not by the old bulge stellar population of the progenitor galaxies. In fact, in agreement with recent stellar measurements (Tacconi et al, 2002), our data suggest that IRAS 17208-0014 is a low mass (i.e. $< m^*$) system.
- 3) The ionized gas emission is concentrated around the optical nucleus, where several luminous star-forming clusters are observed in the *HST* images. Our multi-wavelength analysis indicates that the age of the burst is 5-6 Myr, its mass $3\pm 1 \times 10^8 M_\odot$, and its bolometric luminosity $6\pm 2 \times 10^{10} L_\odot$. This starburst produces only a small fraction of the energy output of IRAS 17208–0014, equivalent to 2.5% of its IR luminosity.
- 4) No strong line emission tracing star-forming regions or tidal-dwarf galaxies are observed in the inner parts of the tidal tails, in contrast with those found in dynamically young double-nuclei ULIRGs. In fact, the secondary nucleus observed in the optical continuum (at 2.7 kpc from the optical nucleus) vanishes at longer wavelengths and does not have distinct kinematics, excluding the possibility of being associated with the nucleus of one of

the merging galaxies.

5) The 2D velocity field has identified the dynamical center of the galaxy as the region coincident with the near-infrared nucleus detected in the NICMOS images. The velocity field also indicates that the 3 kpc inner disk detected in the K-image has a regular rotation pattern ($\Delta V_{\text{circular}} = 250$ km/s). The kinematic and photometric axes are well aligned, which suggests that the stellar and gas components are coupled in this region. No kinematic evidence for a secondary nucleus is found.

6) Radial motions of gas are found along the minor kinematic axis. According to the geometry of the system (fixed by the velocity field and the assumption that the spiral arms-like structures are trailing), the radial motions are well interpreted as inflow perpendicular to the inner disk. The existence of such inflows supports the idea that, as a consequence of the merging process, gas is channeling from the external regions, several kpc away, into the nuclear regions where the massive starburst mentioned above is taking place.

7) The kinematical, morphological and photometric evidence presented here supports the idea that in IRAS 17208-0014 we are witnessing a luminous, cool ULIRG which is at the final coalescence phase of a system composed of two low mass spirals (i.e. $\leq m^*$), with a mass ratio of 2:1, each consisting of a disk+bulge internal structure, that have been involved in a prograde encounter. This system will most likely evolve into a rotating, intermediate-mass ($\sim L^*$) elliptical.

8) All the multifrequency empirical evidence gathered so far indicates IRAS 17207–0014 does not have a luminous QSO nucleus. Starbursts seem to be the dominant energy source and therefore, if an AGN exists, it must produce a minor contribution to the overall energy and ionizing budget. Therefore, IRAS 17208–0014 does not follow the behaviour expected in the 'ULIRG to QSO' evolutionary scenario proposed by Sanders and collaborators. In fact, the present data (as well as those of IRAS 15206+3342; Arribas & Colina, 2002) are in better agreement with the alternative scenario proposed by Colina et al. (2001), according to which cool ULIRGs such as IRAS 17208–0014 are the merger of two low mass ($< m^*$) disk galaxies that will never evolve into a QSO phase.

9) The present study illustrates some caveats to bear in mind when studying high- z dusty galaxies without 2D spectral information at adequate linear resolution. Near and mid-IR integral field spectroscopy is needed to investigate the nature and evolution of luminous infrared galaxies in the early Universe.

We thank all the staff at the Spanish Observatorio del Roque de los Muchachos of the Instituto de Astrofísica de Canarias for their support. We appreciate the careful reading

and comments from Ray Lucas, as well as those from an anonymous referee. Luis Colina thanks STScI for financial support under the Collaborative Visitors Program. We also thank Luis Cuesta by his help using GRAFICOS. Financial support for this work was provided by the Spanish Ministry for Science and Technology through grants PB98-0340-C01, PB98-0340-C02, and AYA2002-01055.

Fig. 1.— Spatial distribution of the spectra in the spectral range 6792 - 7045 Å corresponding to the redshifted H α + [NII] emission line complex. Numbers indicate the fiber/spectrum position at the slit/detector. These spectra are linearly scaled between their lowest and highest values in the represented spectral range.

Fig. 2.— *INTEGRAL* and *HST*/WFPC2 images in the central regions of IRAS 17208-0014. Values for the isolines (in arbitrary units) are: i) H α map: 2.024, 5.402, 11.04, 20.43, 36.11, 62.26, 105.9, 178.6, ii) Continuum map: 0.667, 1.333, 2.00, 2.667, 3.333, 4.00, 4.667, 5.334, 6.00 (contours in the upper-right, lower-left, and lower-right correspond to the same intensity level), iii) H α /[NII] map: 0.443 (blue), 0.914, 1.386, 1.857, 2.328 (white). For the velocity maps, the scale is indicated at the right of each panel. North is at the top and East is to the left.

Fig. 3.— NICMOS K image of IRAS 17208-0014 (first analysed by Scoville et al, 2000), superimposed on the ionized gas velocity field (bottom) and the velocity dispersion map (upper). The values for the isolines are: i) velocity field: 12670, 12711, 12752, 12794, 12835, 12877, 12918, and 12960 km/s, ii) velocity dispersion map: 240, 272, 304, 336, 368, 400 km/s.

Table 1. Ionized gas properties of the optical and near-IR nuclei

Region	A_V^b (mag.)	$F(H\alpha)^c$	$EW(H\alpha)^d$ (Å)	$\log L(H\alpha)^e$ (L_\odot)	$\log([O\ III]/H\beta)^f$	$\log([O\ I]/H\alpha)^f$	$\log([N\ II]/H\alpha)^f$	$\log([S\ II]/H\alpha)^f$
Opt. Nucleus	5.5 ± 0.5	0.56 ± 0.1	94 ± 15	8.55 ± 0.1	-0.002 ± 0.09	-1.60 ± 0.1	-0.40 ± 0.06	-0.51 ± 0.06
					-0.10 ± 0.09	-1.35 ± 0.1	-0.41 ± 0.06	-0.56 ± 0.06
Opt. Nucleus ^(a)	5.4	1.79	51	9.05	-0.16	-1.22	-0.35	-0.54
Near-IR Nucleus	~ 8	0.08	17	8.47		-0.68	-0.07	-0.12

^aAll values taken from Kim, Veilleux, and Sanders (1998) using a slit width of $2''$ along the E–W direction. According to Kim et al. (1995) the uncertainties in the line fluxes are between 5 and 10 %.

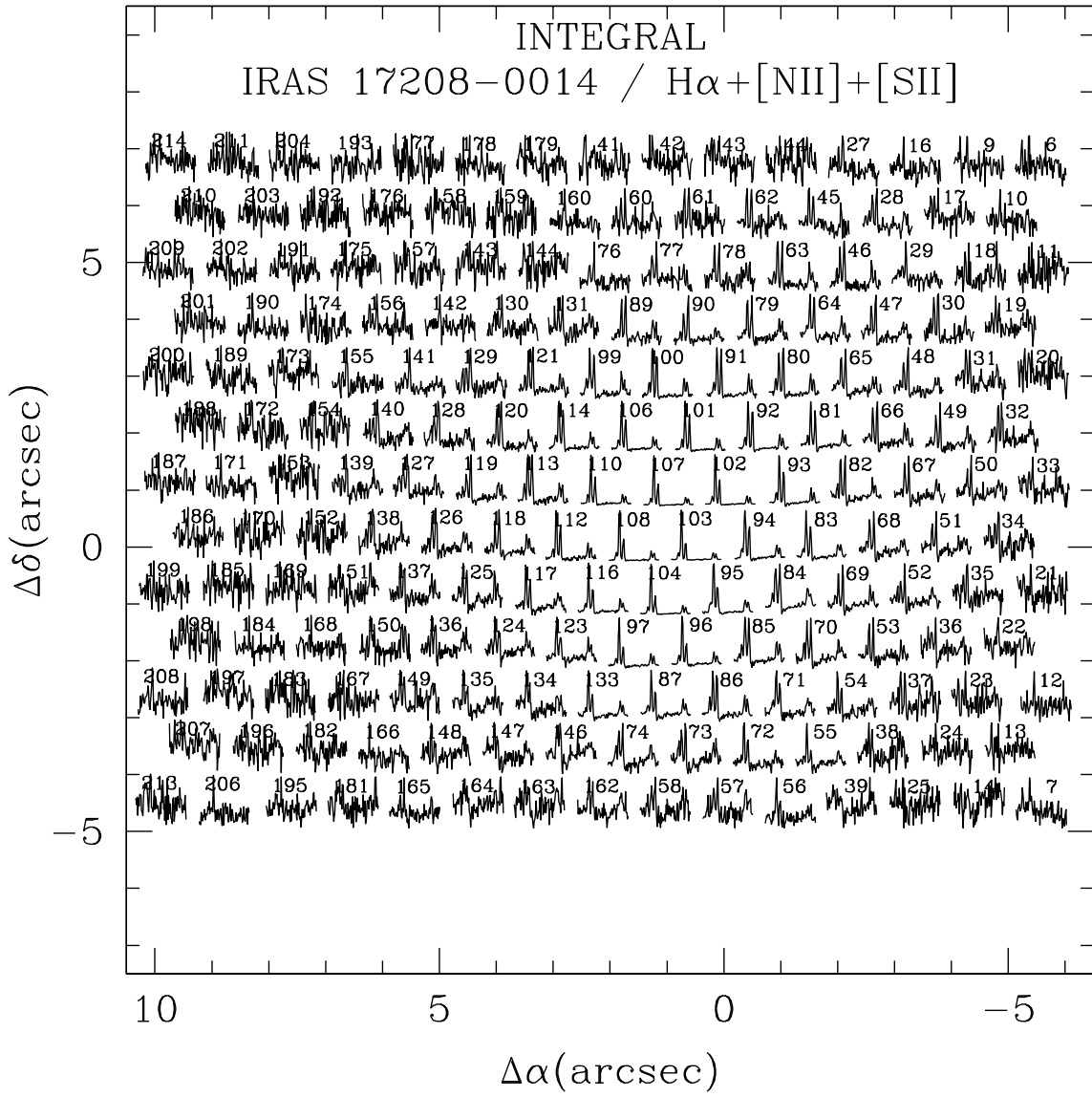
^bInternal extinction derived from the $H\alpha/H\beta$ ratios for the optical nucleus, and from the near-IR colors for the infrared nucleus.

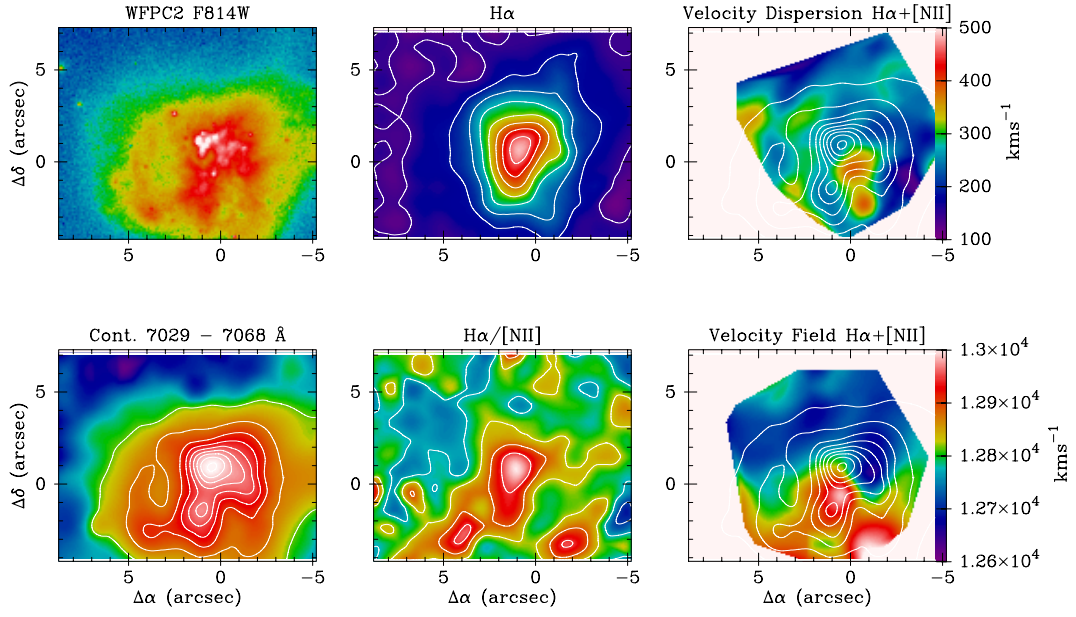
^cObserved $H\alpha$ flux, not corrected for extinction, in units of 10^{-14} erg s^{-1} cm^{-2} . The factor 3.2 discrepancy between the two values listed for the optical nucleus are due to differences in the size of the region. While this work gives the value for the central $1'' \times 1''$, Kim’s value corresponds to a region of $2''$ wide along the E–W direction.

^dThe almost factor 2 discrepancy between the two values for the optical nucleus is due to aperture effects (see above). The larger value represents a more reliable value since it corresponds to a smaller aperture centered on the optical peak emission.

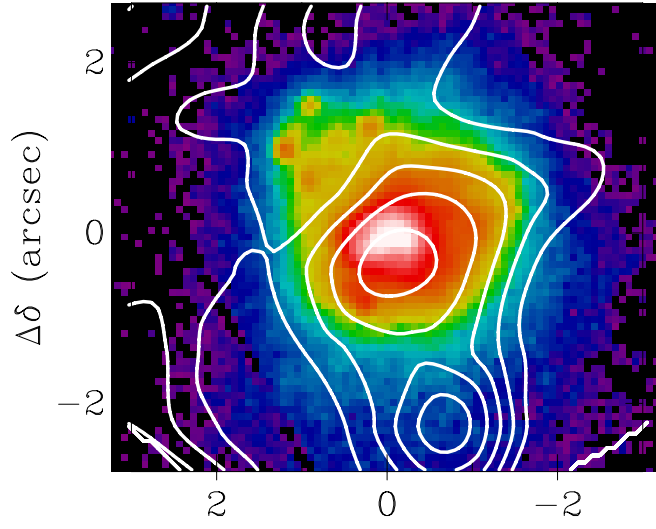
^eExtinction-corrected luminosity using the listed A_V values in units of erg s^{-1} \AA^{-1} .

^fEmission line ratios. First row for our measurements of the optical nucleus presents the observed ratios while the second row gives the extinction-corrected values. The values from Kim et al. are extinction-corrected with the value given in the second column. The ratios for the near-IR nucleus have not been corrected for internal extinction. In addition to the hydrogen Balmer lines, the collisionally-excited lines used are $[O\ III]$ 5007Å, $[O\ I]$ 6300Å, $[N\ II]$ 6584Å, and the $[S\ II]$ doublet 6717,6731Å.

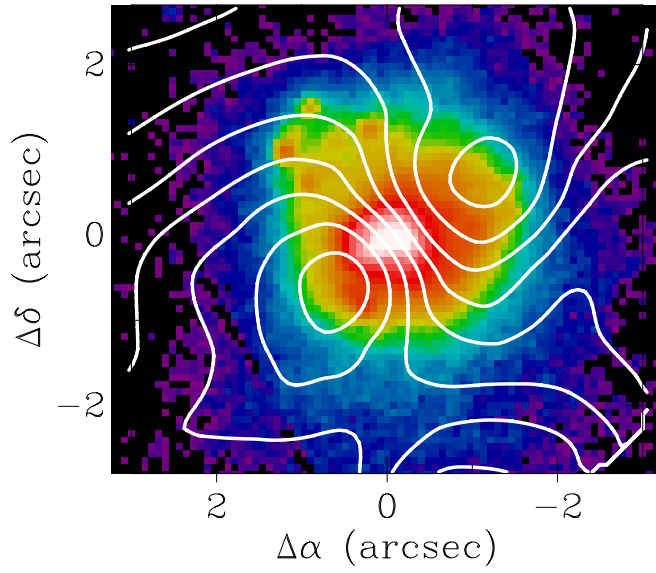




NICMOS-K / Vel. Dispersion



NICMOS-K / Vel. Field



REFERENCES

- Arribas, S., et al. 1998 SPIE, 3355, 821
- Arribas, S., & Colina, L. 2002, ApJ 573, 576
- Arribas, S., Colina, L., & Borne, K. D. 2000, ApJ 545, 228
- Arribas, S., Colina, L., & Clements, D. 2001, ApJ 560, 160
- Arribas, S., & Mediavilla, E. 2000 in 'Imaging the Universe in Three Dimensions: Astrophysics with Advanced Multi-wavelength Imaging Devices', Ed. W. van Breugel and J. Bland-Hawthorn, ASP, Conf. Ser., vol. 195, 295.
- Bingham, R.G., Gellatly, D.W., Jenkins, C.R., Worswick, S.P. 1994, Proc. SPIE 2198, 56
- Bendo, G.J., & Barnes, J. 2000, MNRAS, 316, 315
- Colbert, E.J.W., Baum, S.A., O'Dea, C.P., Veilleux, S. 1998, ApJ, 496, 786
- Colina, L., Arribas, S., & Borne, K. D. 1999, ApJ, 527, L13
- Colina, L., Arribas, S., Borne, K. D., & Monreal 2000, ApJ, 533, L9
- Colina, L., Borne, K., Bushouse, H., Lucas, R.A., Rowan-Robinson, M., Lawrence, A., Clements, D., Baker, A., & Oliver, S. 2001, ApJ, 563, 546
- Condon, J.J., Helou, G., Sanders, D.B., & Soifer, B.T. 1996 ApJS, 103, 81
- Downes, D., & Solomon, P.M. 1998, ApJ, 507, 615
- Dubinski, J., Mihos, J.C., & Hernquist, L. 1999, ApJ 526, 607.
- Duc, P.-A., Mirabel, I.F., Maza, J. 1997, A&AS, 124, 533
- Genzel, R. et al. 1998, ApJ, 498, 579
- Genzel, R., Tacconi, L.J., Rigopoulou, D., Lutz, D., & Tecza, M. 2001, ApJ, 563, 527
- Goldader, J., Joseph, R.D., Doyon, R., & Sanders, D.B. 1995, ApJ, 444, 97
- Heckman, T. M., Armus, L., & Miley, G.K. 1990, ApJS, 74, 833
- Ho, L. et al. 2001, ApJ, 549, L51

- Howarth, I.D., & Murray, J. 1988, DIPSO - A Friendly Spectrum Analysis Program (Starlink User Note 50) (Chilton: Rutherford Appleton Lab.)
- Kim, D.C., Sanders, D.B., Veilleux, S., & Mazzarella, J.M. 1995 ApJS, 98, 129
- Kim, D.C., Veilleux, S., & Sanders, D.B. . 1998, ApJ, 508, 627
- Leitherer, C., Schaerer, D., Goldader, J.D., Gonzalez-Delgado, R.M., Robert, C., Foo Kune, D., de Mello, D., Devost, D., & Heckman, T.M. 1999, ApJS 123, 3
- Lutz, D., Spoon, H.W.W., Rigopoulou, D., Moorwood, A.F.M., & Genzel, R. 1998, ApJ 505, L103
- Lutz, D., Veilleux, S., & Genzel, R. 1999, 517, L13
- Martin, J.M., Bottinelli, L., Dennefeld, M., Gouguenheim, L., & Le Sequeren, A.M. 1989 A&A, 208, 39
- Mediavilla, E., Arribas, S., & Rasilla, J.L. 1991, ApJ, 396, 517
- Mihos, J.C., & Bothun, G.D. 1998, ApJ 500, 619
- Mihos, J.C., & Hernquist, L. 1996, ApJ 464, 641
- Murphy, T.W. et al. 1996, AJ, 111, 1025
- Murphy, T.W., Soifer, B.T., Matthews, K., Armus, L., & Kiger, J.R. 2001, AJ, 121, 97
- Naab, T., & Burkert, A. 2001, in ASP Conf. Ser. 230, Galaxy Disks and Disk Galaxies (ed. J.G. Funes & E.M. Corsini) 451
- Pérez-Olea, D.E., & Colina, L. 1996, ApJ, 468, 191
- Rieke, G.H., & Lebofsky, M.J. 1985 ApJ, 288, 618
- Risaliti, G., Gilli, R., Maiolino, R., & Salvati, M. 2000, A&A, 357, 13
- Sanders, D.B., & Mirabel, I.F. 1996, ARA&A 34, 749
- Sanders, D.B., Soifer, B.T., Elias, J.H., Neugebauer, G., & Matthews, K. 1988, ApJ, 328, L35
- Scoville, N.Z., Evans, A. S., Thompson, R., Rieke, M., Hines, D. C., Low, F. J., Dinshaw, N., Surace, J. A., & Armus, L. 2000, AJ 119, 991

- Soifer, B.T. et al. 2000, AJ, 119, 509
- Solomon, P.M., Downes, D., Radford, S.J.E., & Barrett, J.W. 1997, ApJ, 478, 144
- Surace, J.A., Sanders, D.B., Vacca, W.D., Veilleux, S., & Mazzarella, J.M. 1998, ApJ 492, 116
- Tacconi, L.J., Genzel, R., Lutz, D., Rigopoulou, D., Baker, A.J., Iserlohe, C., & Tecza, M. 2002, ApJ, 580, 73
- Veilleux, S., Kim, D.C., & Sanders, D.B. 1999, ApJ 522, 113
- Veilleux, S., & Osterbrock, D.E. 1987, ApJSS, 63, 295
- Veilleux, S., Kim, D.-C., Sanders, D.B., Mazzarella, J.M., & Soifer, B.T. 1995 ApJS, 98, 171
- Wilman, R. J., Crawford, C. S., & Abraham, R. G. 1999, MNRAS 309, 299